Probabilistic Analysis of the Tsunami Disaster on the Vulnerability Level of Buildings in Painan City, West Sumatra based on the Earthquake Ratio with the Logic Tree Method

Happy King Princes Sitinjak[1*], *Agiel Malik Ibrahim*[1], *Gusti Mahendra Putra*[1], *Teuku Mahlil*[1], *Nurul Fajar Januriyadi*[1] and *Teuku Muhammad Rasyif*[2]

[1]Civil Engineering, Faculty of Infrastructure Planning, Pertamina University, Teuku Nyak Arief Street, South Jakarta, DKI Jakarta, 12220, Indonesia
[2]Civil Engineering, Faculty of Engineering and Computer Science, Bakrie University, Rasuna Epicentrum District, H.R. Rasuna Said Street, Kuningan, DKI Jakarta, 12940

Abstract. Indonesia is an archipelagic country stretching from Sabang to Merauke and is located at the convergence of the most complex and active tectonic plates in the world, namely Eurasia, Indo-Australia, and the Pacific. One of the regions with a high probability of earthquakes and high tsunamis is the island of Sumatra, which lies between the Eurasian and Indo-Australian plates. Painan city is located in West Sumatra Province, where it is surrounded by three megathrust zones: the Nias-Simeulue segment, Mentawai-Siberut segment, and Mentawai-Pagai segment. These three megathrust zones, namely Nias-Simeulue with an estimated earthquake magnitude of 8.7 Mw, Mentawai-Siberut with an earthquake magnitude of 8.9 Mw, and Mentawai-Pagai with an earthquake magnitude of 8.9 Mw, can potentially cause tsunamis that may reach Painan city. The aim of this study is to investigate the influence of seismic activity level variables and the ratio between large and small earthquakes on tsunami wave height using the logic tree method, assess the tsunami hazard potential using Probabilistic Tsunami Hazard Assessment (PTHA), and evaluate the vulnerability of existing buildings in Painan city. Tsunami simulations in this study were conducted using the Cornell Multigrid Coupled Tsunami (COMCOT) program, which applies the Shallow Water Equation (SWE). Additionally, the Building Tsunami Vulnerability (BTV) equation was used to calculate the vulnerability index of buildings based on their conditions and tsunami wave heights. The calculation of the BTV value for the tsunami height parameter was modified using fragility curves that depict the relationship between force and the probability of tsunami wave damage. From the simulation results, the tsunami height was obtained, which in turn determines the probability of tsunami hazard on buildings with return periods of 1000 and 4000 years. After the simulations, the Building Tsunami Vulnerability (BTV) calculation was performed to determine the vulnerability level of buildings to tsunamis.

Keywords: *Probabilistic Tsunami Hazard Assessment, Building Tsunami Vulnerability, Logic Tree, Cornell Multigrid Coupled Tsunami, Painan City.*

1 Introduction

Indonesia is an archipelagic country with an area of approximately 7.81 million km², consisting of land covering around 2.01 million km² (25.7%) and oceans covering about 5.8 million km² (74.3%). It stretches from Sabang to Merauke [1]. Indonesia is situated at the convergence of the most complex and active tectonic plates in the world, namely Eurasia, Indo-Australia, and the Pacific [2]. The disaster potential that Indonesia possesses can threaten its population, including a relatively high earthquake intensity on several islands [3]. Earthquakes and tsunamis are hazardous natural disasters that can occur without warning, delivering significant impacts on human life.

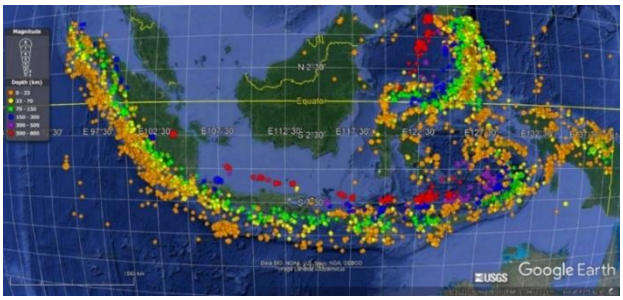

Fig. 1 Earthquake Distribution Map in Indonesia from 2000 to 2021

Indonesia has a marine area covering 74.3%, with many earthquake-prone points visible in **Figure 1** This

* Corresponding author: happykingprinces@gmail.com

region is situated on tectonic plates, which have the potential to trigger natural disasters like tsunamis. Tsunamis can be caused by various disturbances, such as underwater earthquakes, volcanic eruptions, submarine landslides, and celestial object impacts (Rohman, 2019). These disturbances lead to the formation of tsunami waves as the seafloor undergoes changes (disturbance) or vertical shifts in the Earth's crust, resulting in strong shaking and some parts of the seafloor experiencing uplift (subduction). Consequently, the sea undergoes vertical oscillation, launching a series of waves.

West Sumatra, especially the Mentawai Megathrust segment, is a vulnerable area for the collision between tectonic plates and active faults, triggering earthquakes and tsunamis. The segmentation map, particularly of the Mentawai Megathrust fault with a magnitude of 8.9 Mw, is shown in **Figure 2** In 1797, an 8.4 M earthquake occurred. Then, in 1833, a 9 M earthquake followed by a tsunami with a height of 2-3 meters took place [4]. A marine survey conducted in 2008 indicated that the cause of this disaster originated from underwater landslides or backthrust. These events demonstrate that the Mentawai Megathrust segment has significant potential to trigger natural disasters, whether large-magnitude earthquakes or high-height tsunamis.

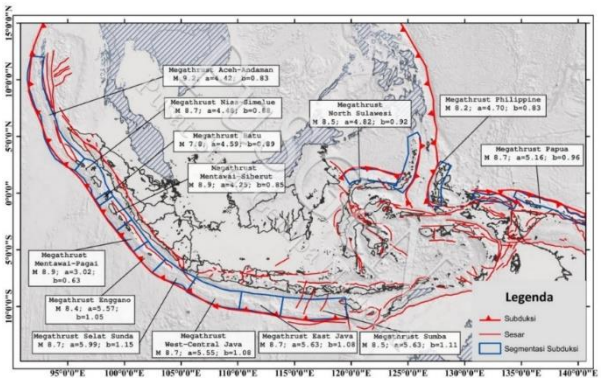

Fig. 2 Indonesia's Segmentation Map and Subduction Mmax

This research employs Probabilistic Tsunami Hazard Analysis (PTHA) as the initial step for assessing tsunami risk and disaster mitigation planning. PTHA is used to assess the hazard of a particular area over a specific time range, with the following fundamental steps: (1) Identifying sources capable of causing tsunamis. (2) Calculating tsunami wave heights through simulations. (3) Determining tsunami hazard curves that connect wave height with return period over a specific timeframe. In this study, a logic tree method is employed to analyze the probability of tsunami heights using variables a and b (seismic activity level and the ratio between major and minor earthquake events) as depicted in **Figure. 2.** set the spacing between the columns at 8 mm. Do not add any page numbers.

This research employs the Cornell Multi-grid Coupled Model (COMCOT) software for conducting tsunami model simulations. COMCOT demonstrates the propagation process of tsunami waves from their generation source to coastal areas, producing tsunami height outputs at specific time intervals [3]. According to [5], COMCOT, created by Yongsik Cho and S.N Seo, is based on theoretical and numerical work conducted by Shuto (1991) and Imamura et al. (1988). COMCOT has achieved numerous successful outcomes, including simulations of the 1960 Chilean Tsunami (Liu et al., 1994) and the 1986 Hua-lien Taiwan Tsunami. Additionally, COMCOT can also be utilized to predict and analyze the impacts of natural disasters, including earthquakes and tsunamis.

The significant losses caused by tsunamis result from a high vulnerability level. Therefore, appropriate mitigation methods are needed to enhance community preparedness. One solution is to utilize strong existing buildings as temporary evacuation sites. If no suitable existing buildings are available, it is recommended to construct vertical evacuation structures in urban areas to facilitate reaching hillside regions. The aim of this research is to assess building vulnerability to tsunami disasters and provide recommendations for facilities and infrastructure to serve as temporary evacuation sites in the event of a tsunami.

2 Research Methods

2.1 Research Sites

The city of Painan, located in West Sumatra Province as shown in Figure 2.1a, is an area with a high seismicity level due to its proximity to the Sumatra Subduction Zone [6]. This condition makes the area susceptible to natural disasters, particularly earthquakes and tsunamis. The tangible evidence of this high risk can be observed from the history of earthquakes along the Sumatra Subduction Zone, such as several major earthquakes in 2004, 2005, 2010, and 2012 with magnitudes of 9.1 Mw, 8.7 Mw, 8.4 Mw, and 7.7 Mw, respectively. The mechanisms of these earthquakes alter the sea surface and generate tsunamis, resulting in damage to infrastructure, agricultural land, flooding in low-lying areas, and loss of lives.

Moreover, near the capital of West Sumatra Province, Padang, there is also evidence of a seismic gap, an area that has not experienced a major earthquake, thus accumulating seismic energy that could lead to future earthquakes and tsunamis with a recurrence period of around 200 years [7]. **Figure 3** represents the Painan city area with a size of 2.49 km² and a population of around

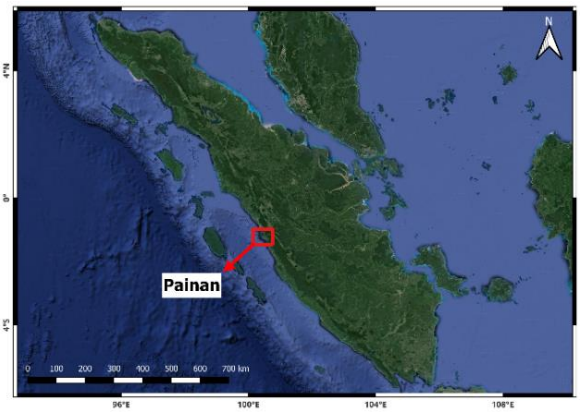

Fig. 3 Area Study

5,888 people, with a population density of about 2,365 people per km² in 2021, as reported by the [8].

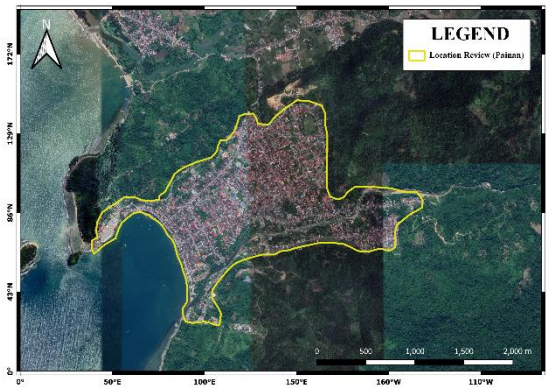

Fig. 4 BTV analysis was carried out at the Review Locations

2.2 Building Classification

In this current research, the classification data of buildings in Painan City were obtained from a survey previously conducted by [9]. **Figure. 5** displays the distribution map of buildings based on building class in Painan City. Additionally, **Table 1.** presents the number of buildings in Painan City. These visuals illustrate the class zones related to the building conditions, which can be categorized based on the constituent materials and the number of floors for Reinforced Concrete (RC) buildings. According to [10], the purpose of classifying the number of floors for RC buildings is to identify which structures can serve as evacuation sites in the event of a tsunami disaster.

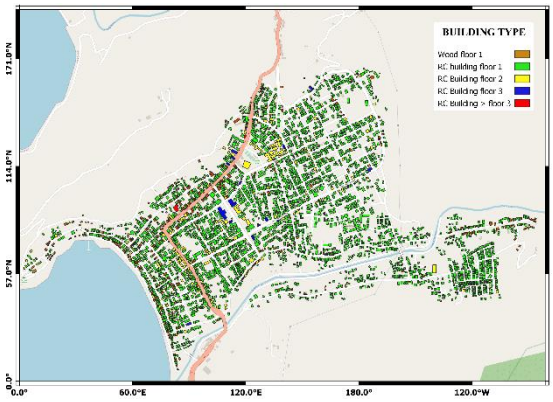

Fig. 5 Map of Building Distribution Based on Building Class in Painan City

Table 1. Number of Buildings according to Building Class (Fc,b) in Painan City

Building Type	Zone Class	*Building Class* (Fc,b)	Amount (units)	Amount (%)
Wood floor 1	A	5	417	10.76
RC *building* fl.1	B	4	3198	82.48
RC *building* fl.2	C	3	241	6.22
RC *building* fl.3	D	2	19	0.49
RC *building* > fl.3	E	1	2	0.05
		Total	3876	100

2.3 Numerical Modeling

In this study, simulations for tsunami waves were conducted using the Cornell Multi-grid Coupled Tsunami (COMCOT) program, employing a 2-Dimensional Horizontal (2DH) modeling approach. The COMCOT program has achieved successful simulations with accurate and efficient outcomes, as seen in cases such as the Chilean tsunami (1960), Indonesian tsunamis (2004, 2005, and 2006), and the Japanese tsunami (2011). This program is capable of numerically simulating tsunami waves, thus generating the propagation of tsunamis from the earthquake's epicenter to coastal areas using the Shallow Water Equations (SWE), which encompass equations of momentum and mass conservation. Subsequently, discretization is conducted using the leapfrog and upwind methods. The SWE equations are discretized in space and time for linear and nonlinear equations in both spherical and Cartesian coordinates. The SWE equations can be formulated as follows [5].

$$\frac{\partial \eta}{\partial t} + \frac{1}{R\cos\varphi}\left\{\frac{\partial P}{\partial \psi} + \frac{\partial}{\partial \varphi}(\cos\varphi Q)\right\} = 0 \quad (1)$$

$$\frac{\partial P}{\partial t} + \frac{1}{R\cos\varphi}\frac{\partial}{\partial \psi}\left\{\frac{P^2}{H}\right\} + \frac{1}{R}\frac{\partial}{\partial \psi}\left\{\frac{PQ}{H}\right\} + \frac{gH}{R\cos\varphi}\frac{\partial \eta}{\partial \psi} - fQ + F_x = 0 \quad (2)$$

$$\frac{\partial Q}{\partial t} + \frac{1}{R\cos\varphi}\frac{\partial}{\partial \psi}\left\{\frac{PQ}{H}\right\} + \frac{1}{R}\frac{\partial}{\partial \varphi}\left\{\frac{Q^2}{H}\right\} + \frac{gH}{R}\frac{\partial \eta}{\partial \varphi} + fQ + F_x = 0 \quad (3)$$

Where η represents the water surface elevation. t stands for time. R is the Earth's radius. φ and ψ denote the latitude and longitude coordinates of the Earth. P and Q are flux volumes in the x and y directions. g is the Earth's gravitational acceleration. $H = h + \eta$ signifies the total water depth, where h is the water depth. f is the coefficient of Coriolis force due to Earth's rotation. Fx and Fy represent bottom friction in the x and y directions.

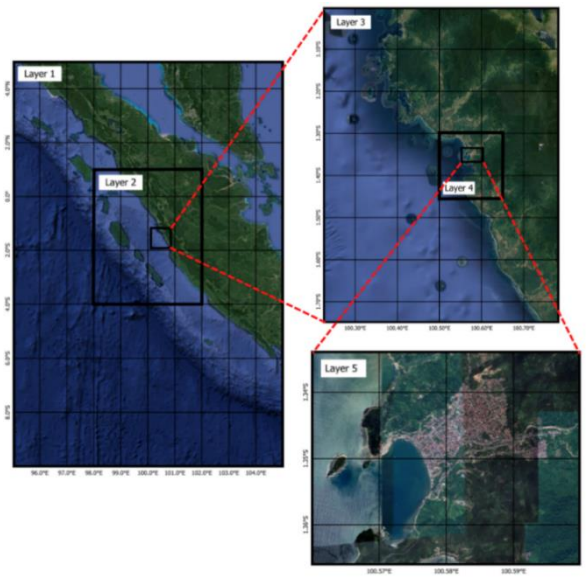

Fig. 6 Form of Multilayer Area Simulation in the COMCOT Program

Figure 6 illustrates a multilayer system created to encompass the area needed for performing tsunami wave simulations in Painan City. The purpose of employing a multilayer approach in this simulation is to model tsunami

waves with smaller grid sizes in specific focus areas of the study, namely in Painan City. A total of five layers are utilized. Equations applied in layers 1 through 4 involve spherical coordinates (accounting for Earth's curvature), while layer 5 employs Cartesian coordinates (disregarding Earth's curvature/having closer distances). Parameters used for the simulation area coverage are provided in **Table 2** Topographic and bathymetric data used across all layers originate from the BATNAS (National Bathymetry) and DEMNAS (National Digital Elevation Model) sources.

Table 2 Simulation parameter information for the COMCOT program

Domain	Layer 1	Layer 2	Layer 3
Latitude (°)	95E-105E	98E-102E	100,25E-100,75E
Longitude (°)	10S-5N	4S-1N	1,75S-1S
Size grid (m)	1850	370	74
Total grid	600×900	1200×1500	750×1125
Parent grid	-	*Layer* 1	*Layer* 2
Ratio to parent grid	-	5	5
Coord. System	*Spherical*	*Spherical*	*Spherical*
SWE *type*	*Linear*	*Linear*	*Linear*
Time step (second)	1	1	0,333
Manning's roughness coef		0,02	

Domain	Layer 4	Layer 5
Latitude (°)	100,5E-100,65E	100,55E-100,6E
Longitude (°)	1,45S-1,3S	1,37S-1,34S
size grid (m)	14,8	2,96
Total grid	1125×1125	1907×1147
Parent grid	*Layer* 3	*Layer* 4
Ratio to parent grid	5	5
Coord. System	*Spherical*	*Spherical*
SWE *type*	*Linear*	*Nonlinear*
Time step (second)	0,333	0,083
Manning's roughness coef	0,02	

2.4 Initial Conditions

When conducting simulations using the COMCOT program, the input data consists of earthquake mechanism data. In this study, the triggering mechanism for generating tsunami waves in the Padang fault zone is underwater plate sliding. The earthquake mechanism data input in this research utilizes stochastic slip modeling. The approach taken is based on the work by Mei & Beroza (2002), where they developed a method to characterize slip complexity in earthquakes, relying on spatial random fields of anisotropic wavenumber spectrum with a Von Karman autocorrelation function.

For the Padang Fault, the slip modeling employs a fault length and width of 600 km and 240 km, respectively. This fault is divided into multiple smaller fault areas, each measuring 10 × 10 km. The earthquake depth, strike, rake, and dip values utilized are 40 km, 325°, 75°, and 13°, respectively, based on [11]. On the other hand, for the Nias-Simeulue Fault, data is used with a fault length and width of 700 km and 200 km, respectively. The earthquake depth is set at 20 km, and strike values (315°, 320°, 325°, and 330°), dip values (10° and 20°), and rake values (95° and 107°) are based on the prior study by [12].

Furthermore, for the Bengkulu Fault, data is employed with a fault length and width of 640 km and 140 km, respectively. The earthquake depth, strike, rake, and dip values are 34 km, 323°, 103°, and 11°, respectively. The scenario used involves earthquakes with magnitudes ranging from 8.5 to 9 in intervals of 0.1. Each earthquake interval consists of 100 scenario cases. Hence, the total number of scenarios used is 600 scenarios.

2.5 Probabilistic Tsunami Hazard Assessment (PTHA)

The primary goal of hazard assessment is to estimate the extent of danger posed by an event and the resulting level of risk. According to [13], there are two methods for conducting hazard assessment: deterministic and probabilistic. The deterministic method is used to measure the magnitude of hazard based on past occurrences. On the other hand, the probabilistic method is employed to assess hazard by considering all potential events that could occur.

In this research, the probabilistic method is employed to assess future tsunami hazards. This method is also known as PTHA (Probabilistic Tsunami Hazard Assessment), which is used to determine the level of hazard risk for a specific area over a certain period. This method involves fundamental steps that need to be undertaken: (1) Determining source parameters; in this study, earthquake sources from the Padang fault, Nias-Simeulue fault, and Bengkulu fault are used. (2) Calculating tsunami wave heights at each building location by simulating tsunami propagation from the earthquake sources using the numerical simulation program COMCOT. (3) The simulation results yield tsunami hazard curves at the evaluated locations. PTHA is fundamentally characterized by the following equation.

$$\lambda(H \geq c) = \sum_{i=1}^{n_s} v_i \sum_{j=1}^{n_m} P\left(H \geq c | m_j\right) P(M_i = m_j) \quad (4)$$

Where c is the testing tsunami wave height, H is the simulated tsunami wave height. Ns stands for the total number of sources/faults (i), nm is the number of magnitudes m considered with interval (j). This study

considers a range of magnitudes from the smallest magnitude Mmin to the largest magnitude Mmax with an interval of 0.1. λ represents the earthquake occurrence rate per year. P is the probability percentage of occurrence at a specific return period. Mj signifies the magnitude of the earthquake utilized.

Then, when calculating PTHA using varying β values based on a logic tree, the logic tree values have been established by [14]. The β value is the cumulative standard normal distribution equation. In the equation, the β value is ln(κ) as shown below, and determining this value has been carried out by [15].

2.6 Modified Damage Probability

Another parameter in the building vulnerability study, apart from building conditions, is the damage probability parameter. According to [16], damage probability determines the likelihood of structural damage to buildings caused by a tsunami disaster, employing approaches such as hydrodynamic force, inundation depth, and velocity. This study produced a fragility function for buildings affected by the 2004 tsunami in Banda Aceh. The initial formula for damage probability against tsunamis proposed by [16] has been modified using tsunami wave height values based on specific return periods through the PTHA method, as seen in the Equation below (5) .

$$P(x_i) = \Phi\left[\frac{x_i-\mu}{\sigma}\right] \quad (5)$$

Where x_i represents the tsunami wave height for a specific return period. Φ is the standardized lognormal distribution function with mean (μ) and standard deviation (σ) values of 2.99 and 1.12, respectively.

2.7 *Building Tsunami Vulnerability* (BTV)

The Building Tsunami Vulnerability (BTV) is a method used to determine the index value of tsunami vulnerability and identify locations highly susceptible to tsunamis. This aids in mapping the research areas into categories of high, medium, and low risk levels [17]. When using BTV for analysis, three parameters are considered: building conditions, tsunami height, and coastal defense [18]. The coastal defense parameter is not utilized in this study due to the absence of coastal protection in the coastal area of Painan city, which makes this parameter not significantly variable. In this research, the tsunami height parameter is modified to become damage probability based on tsunami wave height for specific return periods. The damage probability parameter is better suited to represent the vulnerability of buildings to tsunami disasters [10]. The equation used can be seen in Equation (2.6).

$$BTV_i = \frac{(Fc,b \times Fw,b)+(Fc,d \times Fw,d)}{\sum_{(k=1)}^{2}(Fc,max \times Fw)k} \times 100\% \quad (6)$$

Where BTV_i represents the building tsunami vulnerability for a specific return period. Fc,b is the classification factor for building conditions. Fw,b is the weighting factor for building types with a value of 2 (two). Fc,d is the classification factor for building collapse based on damage probability for a specific return period. Fw,d is the weighting factor for building collapse probability with a value of 1 (one). **Table 3** below illustrates the BTV classification used. Using the modified BTV equation because it incorporates damage probability levels from "none" to "very high" for building destruction, while in previous research, only the tsunami height was considered during the BTV analysis.

Table 3 Building type factor, damage probability, and BTV Classification

Building Type Factor ($F_{c,b}$)

Building Type	$F_{c,b}$
Wooden Building (1 Floor)	5
Reinforced Concrete Building (1 Floor)	4
Reinforced Concrete Building (2 Floor)	3
Reinforced Concrete Building (3 Floor)	2
Reinforced Concrete Building (>3 Floor)	1

Probability damage factor ($F_{c,d}$)

$P(x_i)$	$F_{c,d}$
$P(x_i) \geq 0.8$	5
$0.6 \leq P(x_i) < 0.8$	4
$0.4 \leq P(x_i) < 0.599$	3
$0.2 \leq P(x_i) < 0.399$	2
$0.001 \leq P(x_i) < 0.199$	1
$P(x_i) = 0$	*Not affected*

BTV Classification

BTV (%)	Classification
$BTV_i \geq 80$	*Very High*
$60 \leq BTV_i < 80$	*High*
$40 \leq BTV_i < 60$	*Medium*
$20 \leq BTV_i < 40$	*Low*
BTV < 20	*None*

3 Results and Discussion

3.1 *Initial Condition*

To understand the initial occurrence of a tsunami from its source location, an initial condition is utilized. This initial condition data is obtained through the slipreal program by applying stochastic slip modeling. In this modeling approach, earthquake magnitudes used for simulations range from 8.5 Mw to 9 Mw. Each earthquake magnitude is tested with 100 different scenarios due to variations in slip values across scenarios. Consequently, a total of 600 scenarios are employed in this study. The initial condition used with a magnitude of 9.0 Mw in this research is shown in **Figure 7** (Padang fault), indicating differences in the initial tsunami generation conditions between scenario 1 (**Figure 7a**) and scenario 50 (**Figure 7b**). These variations arise from the different slip values generated for each scenario.

The red colour represents the rise in sea surface caused by the uplift of the seafloor. This uplift of the seafloor is determined by calculating slip values using the SlipReal program. Due to the seafloor uplift, the sea surface also rises, leading to a decrease in sea surface (blue colour) as observed in **Figure 7**. The type of fault utilized is a reverse fault, occurring when the hanging wall moves upwards relative to the footwall. To determine the fault type to be used, it is advised to refer to the USGS website first, where the fault type can be visualized in the form of a beachball diagram.

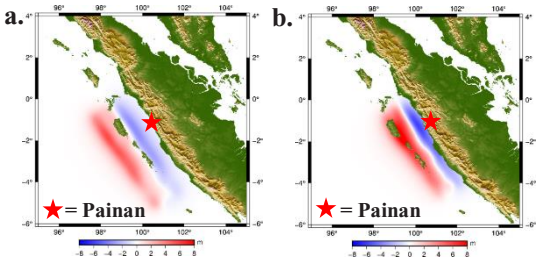

Fig. 7 Initial Condition with an earthquake strength of 9.0 Mw for an earthquake scenario: a. 1 and b. 50

In **Figure 7**, a distinction is visible where the faded areas have a broader extent compared to the darker areas, resulting from the constraint imposed on the sum of slip values not exceeding the energy limit for the specified moment magnitude. For this study, it is not feasible to determine a specific constraint for seafloor uplift. Thus, the energy constraint (Mo) as established by Hanks and Kanamori in 1979 for each moment magnitude is employed. Therefore, the SlipReal program is used to acquire slip values, as investigated by [19].

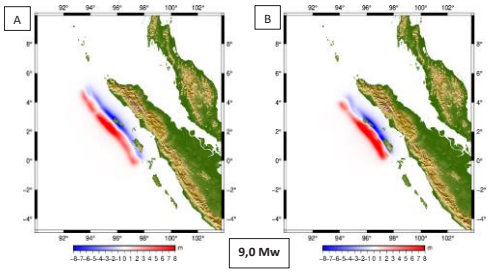

Fig. 8 Initial Conditions with Mw 9 : (a) scenario 99 and (b) scenario 100

In **Figure 8** (Nias-Simeulue fault), a moment magnitude of 9.0 Mw is used. A moment magnitude of 9.0 Mw is the largest magnitude employed in this study. It can be observed that the area experiencing uplift and subsidence becomes more extensive. At a magnitude of 9.0 Mw, the maximum and minimum elevations range from -7 m to -8 m for the minimum and from 7 m to 8 m for the maximum.

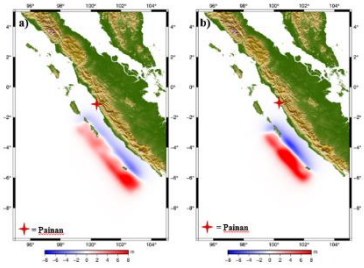

Fig. 10 Initial Conditions with Mw 9 : (a) scenario 1 and (b) scenario 10

In **Figure 9** (Bengkulu fault), the initial condition at a magnitude of 9.0 can be observed in **Figure 9a** for scenario 1 and **Figure 9b** for scenario 10. From the figures, it is evident that in scenario 1, the sea level experiences an increase reaching a height of 7 - 8 meters and subsequently decreases to -5 meters. On the other hand, in scenario 10, the sea level rises by 8 meters and then decreases to -7 meters.

3.2 Process of Tsunami Wave Propagation

After conducting simulations using COMCOT, the next step involves simulating the propagation from layer 1 to layer 5 with earthquake magnitudes ranging from 8.5 to 9 Mw. Selecting scenarios, earthquake magnitudes, and layers to be displayed randomly to determine the tsunami wave height and the subsequent sea level drop caused by the earthquake originating from its source. The propagation of the tsunami wave, which will be depicted in visualizations, includes a magnitude 9.0 Mw earthquake on the Padang fault, scenario 50, and focuses on layer 1, representing the initial conditions of the tsunami's occurrence from the source (fault), as well as layer 5, representing the coastal and inland areas of Painan city.

The simulations using the COMCOT program were conducted for 120 minutes (7200 seconds) with data results recorded every 4 minutes (240 seconds). **Figure 10** illustrates the tsunami wave propagation process in layer 5. The tsunami wave begins to reach the coastal area in just 12 minutes from the earthquake source. By the 36 minute, the maximum tsunami wave height reaches 20 meters, with an inundation distance of over 1.5 kilometers. At the location of the Bank Nagari Branch Office marked with ☆, as shown in **Figure 11**, the tsunami height is approximately 13 meters. This building is a 4-story reinforced concrete structure with a total height of 20 meters. Hence, this building can serve as a Temporary Evacuation Site for the community. Subsequently, the tsunami wave recedes by the 120 minute.

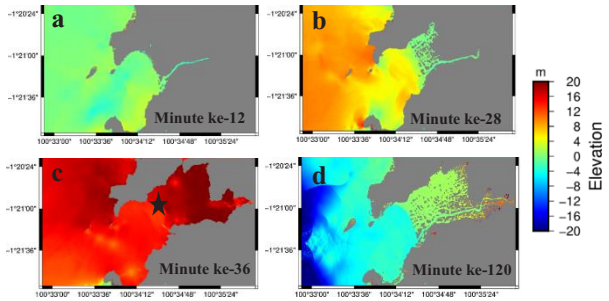

Fig. 11 Tsunami propagation process in layer 5 for: a)t=12 minutes, b)t=28 minutes, c)t=36 minutes, and d)t= 120 minutes

Fig. 9 Nagari Bank Branch Office

3.3 Probabilistic Tsunami Hazard Assessment (PTHA)

The Probabilistic Tsunami Hazard Assessment (PTHA) is employed to determine the probability of various tsunami wave heights occurring for each magnitude of an earthquake, as well as to establish the annual rate of occurrences (λ) to derive return period values. In the stages of PTHA analysis, several critical data points are necessary. Using three scenarios for values of "a" and "b", these values are obtained based on PUSGEN & PUSLITBANG PUPR, 2017. The values of "a" and "b" are then employed through addition and subtraction. Moreover, hazard curves are generated for each building based on the potential tsunami wave heights. These curves compare the projected water height, the annual rate of exceedance (λ), and the return period (t).

"When analyzing PTHA, the return period value obtained is influenced by the 'a' and 'b' values on the segmentation map. These values are highly sensitive, so it can be said that the 'a' and 'b' values are still under study. In this research, these return period values are used when conducting PTHA analysis, with the smallest return period value obtained from the minimum tsunami height considered."

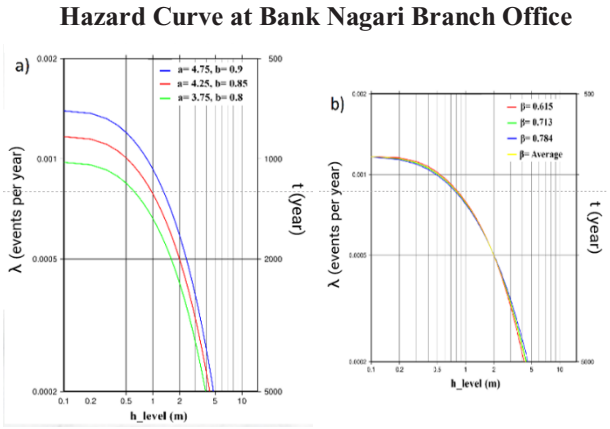

Fig. 14 Tsunami height value at Bank Nagari Branch Office; a) variations in the values of a and b, b) the value of the variation of β based on the hazard curve

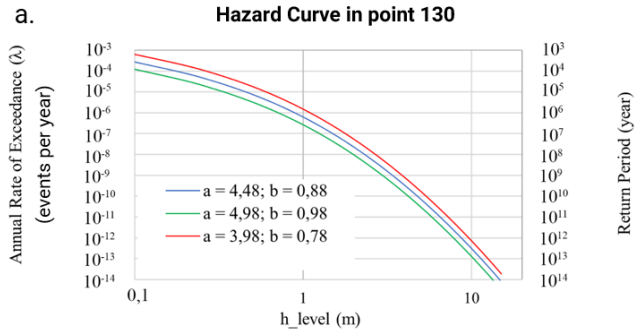

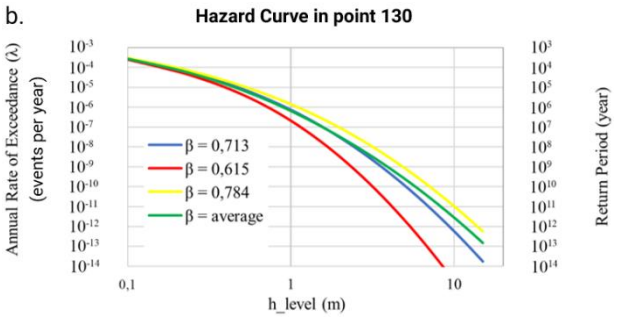

Fig. 12 Comparison of Hazard Curves based on: a.Value a and Value b, b.Logic Tree (β)

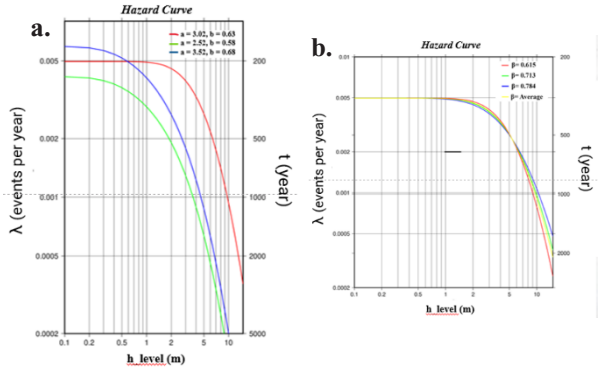

Fig. 13 Comparison of Hazard Curves based on: a.Value a and Value b, b.Logic Tree (β)

Figure 12a represents the hazard curve for the Padang fault, **Figure 13a** depicts the Nias-Simeulue fault, and **Figure 14a** illustrates the Bengkulu fault with varying values of "a" (seismic activity level) and "b" (ratio of large to small earthquake events). A little information for **Figure 13** and **Figure 14**, they represent hazard curves that examine buildings located around the coastal area due to the region being affected by tsunami impacts, compared to **Figure 12**, which represents Bank Nagari buildings that are located closer to the city center.

It can be observed in the figures that the graphs are highly sensitive to different values of "a" and "b". The red curve in these figures corresponds to the values from the PUSGEN dataset. It is evident that for a return period of 1000 years, with "a" value of 3.75 and "b" value of 0.8, the wave height does not reach 0.1 meters.

If the natural disaster has never occurred before, then the value of β used can be random. In **Figure 12b** below, the resulting hazard curve is shown when changing the value of β. It can be observed from the curve that the obtained values of λ and t are not significantly affected when using different values of "a" and "b". Sensitivity to the use of β values also leads to differences in tsunami wave height; when using the smallest β value of 0.615 and the largest β value of 0.718, the wave height can reach up to 1.7 meters.

3.4 Damage Probability

According to [16], damage probability refers to determining the likelihood level of structural damage to buildings caused by a tsunami disaster, using hydrodynamic force, inundation depth, and velocity approaches. In this study, the approach is focused on inundation depth. The resulting inundation caused by the calculation of damage probability is based on the tsunami height at each building location. In its calculation, damage probability employs The Standardized Lognormal Distribution Functions with input data such as mean (μ) and standard deviation (σ), obtained from research previously conducted by [16].

Table 4 Damage Probability based on the number of buildings and classes (Fc,d) in Painan City in the return period of 1000 years and 4000 years (Padang Fault)

Damage Probability	Fc,d	Damage Type	1000 Year		4000 Year	
			Amount (Unit)	Amount (%)	Amount (Unit)	Amount (%)
>0.8	5	*Total Collapse*	16	0.41	2989	69.56
0.6 – 0.8	4	*Heavy Damage*	1	0.03	288	7.43
0.4 – 0.599	3	*Moderate Damage*	1	0.03	164	4.23
0.2 – 0.399	2	*Minor Damage*	29	0.75	157	4.05
0.001 – 0.199	1	*Non-Structural Damage*	3211	82.84	356	9.18
0	0	*Not Affected*	618	15.94	215	5.55
		Total	3876	100	3876	100

As seen in the **Table 4** above, there is a number of buildings classified based on their damage probability values for the return periods of 1000 and 4000 years. For the 1000-year return period, there are 618 building locations, and for the 4000-year return period, there are 215 building locations with a damage probability class value of 0. This indicates that these points are not affected by the tsunami waves reaching the buildings since the inundation doesn't reach them. There are also 16 building locations for the 1000-year return period and 2989 building locations for the 4000-year return period with a damage probability class value of 5. This implies that the buildings at these locations have a probability level with the maximum impact based on inundation height. For the 4000-year return period, there is an increase in the percentage of the total number of buildings falling into classification 5, and the value of damage probability >0.8 is 69.15%.

Table 5 Damage Probability based on the number of buildings and classes (Fc,d) in Painan City in the return period of 500 years and 2000 years (Bengkulu fault)

Damage Probability	Fc,d	Damage Type	500 Year		2000 Year	
			Amount (Unit)	Amount (%)	Amount (Unit)	Amount (%)
>0.8	5	*Total Collapse*	15	0.39	5	0.13
0.6 – 0.8	4	*Heavy Damage*	0	0	3	0.08
0.4 – 0.599	3	*Moderate Damage*	0	0	4	0.10
0.2 – 0.399	2	*Minor Damage*	0	0	4	0.10
0.001 – 0.199	1	*Non-Structural Damage*	30	0.77	97	2.50
0	0	*Not Affected*	3831	98.84	3763	97.09
		Total	3876	100	3876	100

Based on **Table 5**, it can be observed that the tsunami waves originating from the Bengkulu fault have relatively low impact on Painan city. This can be seen in the number of buildings with a damage probability value classified as class 0, which is around 97-98% for return periods of 500 and 2000 years. In this context, the damage probability within class 0 falls under the "not Affected" damage type, signifying that these buildings are not affected by the impact of the tsunami waves.

3.5 Building Tsunami Vulnerability (BTV)

The classification of BTV classes follows the research conducted by [10]. When performing Building Tsunami Vulnerability (BTV) analysis, input data in the form of building condition classes, as determined by the study of [9], and inundation classes obtained from damage probability calculations are required. The results of the Building Tsunami Vulnerability calculation for each building in Painan city and also for each fault can be seen in the table below.

Based on the information contained in **Table 6**, it can be concluded that the highest number of buildings with a high vulnerability level is predominantly found in the BTV class during the 1000-year recurrence period. There are a total of 2974 building units classified as BTV 3, which constitutes 76.73% of the total number of buildings in Painan City. This means that approximately 76.73% of the buildings in Painan City have a high probability of experiencing severe damage. For the 4000-year recurrence period, buildings classified as BTV 4 (very high) have the highest number. There are a total of 2752 building units included in the BTV 4 class, representing 71% of the total buildings in Painan City.

Table 6 BTV Class Calculation Results in Painan City in 1000 Years and 4000 Years Return Period (Padang Fault)

BTV *Class*	BTV (%)	*Vulnerability*	1000 Year		4000 Year	
			Amount (Unit)	Amount (%)	Amount (Unit)	Amount (%)
4	>80	*Very High*	26	0.67	2752	71
3	60-80	*High*	2974	76.73	892	23.01
2	40-60	*Normal*	234	6.04	13	0.34
1	20-40	*Low*	21	0.54	0	0
0	0-20	*None*	621	16.02	219	5.65
Total			3876	100	3876	100

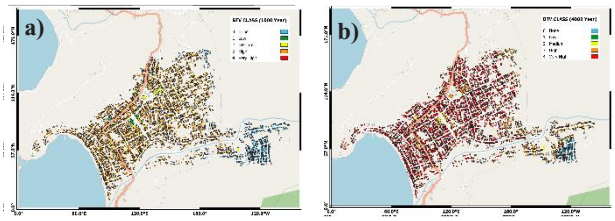

Fig. 15 Map of Building Vulnerability Distribution Based on Recurrence Period of: a)1000 Years and b)4000 Years

In the **Table 7** below, it can be observed that for a recurrence period of 10,000 years, 2.45% of the buildings in Painan City exhibit a low level of damage, while the remaining 97.55% of other buildings show no damage due to tsunamis generated by the Nias-Simeulue fault. The 2.45% of buildings with low damage levels are located in the northwestern part of Painan City.

Table 7 BTV Class Calculation Results in Painan City in 10000 Years Return Period (Nias-Simeulue fault.)

BTV *Class*	BTV (%)	*Vulnerability*	10000 Year	
			Amount (Unit)	Amount (%)
4	>80	*Very High*	0	0
3	60-80	*High*	0	0
2	40-60	*Normal*	0	0
1	20-40	*Low*	95	2.45
0	0-20	*None*	3781	97.55
Total			3876	100

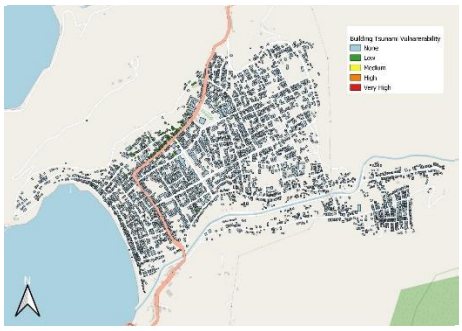

Fig. 16 Map of Building Vulnerability Distribution Based on Recurrence Period of 10000 Years

Based on **Table 8**, it can be observed that the number of buildings with a very high vulnerability level is 17 units, the number of buildings with a high vulnerability level is 77 units, and the number of buildings with a normal vulnerability level is 4 units for the 500-year recurrence period. Meanwhile, for the 2000-year recurrence period, the number of buildings with a very high vulnerability level is 12 units, the number of buildings with a high vulnerability level is 92 units, and the number of buildings with a normal vulnerability level is 7 units. However, the number of buildings without vulnerability to tsunami waves for the 500 and 2000-year recurrence periods is not significantly different, approximately comprising 97% of the total number of buildings.

Table 8 BTV Class Calculation Results in Painan City in 500 Years and 2000 Years Return Period (Bengkulu Fault)

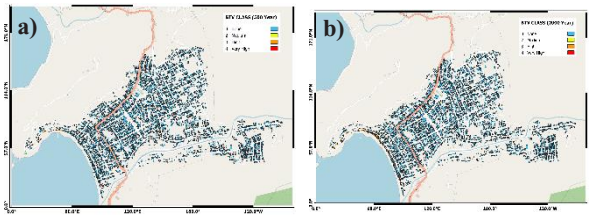

Fig. 17 Map of Building Vulnerability Distribution Based on Recurrence Period of: a)500 Years and b)2000 Years

BTV *Class*	BTV (%)	*Vulnerability*	500 Year		2000 Year	
			Amount (Unit)	Amount (%)	Amount (Unit)	Amount (%)
4	>80	*Very High*	17	0.44	12	0.31
3	60-80	*High*	77	1.99	92	2.37
2	40-60	*Normal*	4	0.10	7	0.18
1	20-40	*Low*	0	0	0	0
0	0-20	*None*	3778	97.47	3765	97.14
Total			3876	100	3876	100

4 Conclusion

The influence of varying variable a (seismic activity level) and variable b (ratio between large earthquakes and small earthquakes) in analyzing PTHA (Probabilistic Tsunami Hazard Analysis) can be seen in the hazard curve based on the different values of a and b. The comparison of each of these values shows significant differences in the resulting annual rate of exceedance (λ) and return period (t). On the other hand, when using variable β (which varies) with a logic tree, the hazard curve obtained shows insignificant differences compared to variables a and b. This implies that variables a and b exhibit a sensitive nature when incorporated into PTHA analysis and altered.

The potential hazard posed by tsunami disasters in Painan City is very high due to earthquakes along the Padang Fault Zone. The results of the PTHA analysis provide information regarding tsunami height at each building with predetermined recurrence periods. There is a probability of maximum tsunami height along the Padang fault reaching 36 meters for a 1000-year recurrence period, and 5,665 meters for a 4000-year recurrence period. For the Nias-Simeulue fault, during a 10,000-year recurrence period, at least one tsunami wave with a height ranging from 0 to 0.45 meters is expected to occur at several observation points. Additionally, concerning the Bengkulu fault, there is a probability of maximum tsunami height along the fault reaching 1 meter for a 200-year recurrence period.

One of the ways to mitigate the impact caused by tsunami disasters, based on the building's vulnerability to tsunamis (Building Tsunami Vulnerability), is by utilizing buildings with a Building Tsunami Vulnerability (BTV) level of 0 (none), 1 (low), and 2 (medium). It can be observed in the BTV analysis for the 4000-year recurrence period along the Padang fault that due to the potential reach of tsunami waves onto the city of Painan's land, coastal residents can seek refuge at the Branch Office of Bank Nagari in the event of a disaster. This is because the location is suitable for use as an evacuation site. The distance of this location from the areas around the coastline is approximately 460 meters, and it has the capacity to accommodate 500-700 people.

References

[1] O. Pratama, "Konservasi Perairan Sebagai Upaya menjaga Potensi Kelautan dan Perikanan Indonesia," *DIREKTORAT JENDERAL PENGELOLAAN RUANG LAUT*, 2020. https://kkp.go.id/djprl/artikel/21045-konservasi-perairan-sebagai-upaya-menjaga-potensi-kelautan-dan-perikanan-indonesia#:~:text=Dari total luas wilayah tersebut,juta km2 yang berupa daratan.

[2] A. Mega, "PEMODELAN MITIGASI BENCANA TSUNAMI DI PANTAI LOSARI," *Inst. Teknol. SEPULUH Novemb.*, 2018.

[3] E. S. Ratuluhain, I. W. Nurjaya, and N. M. N. Natih, "ANALISIS POTENSI TSUNAMI DI LOMBOK UTARA," vol. 13, no. April, pp. 113–126, 2021.

[4] Badan Nasional Penanggulangan Bencana, "Refleksi Tsunami 1797," *bnpb.go.id*, 2020. https://bnpb.go.id/berita/refleksi-tsunami-1797

[5] X. Wang, "COMCOT User Manual Ver. 1.7," in *Cornell University*, vol. 6, 2009, pp. 1–59.

[6] R. McCaffrey, "The Tectonic Framework of the Sumatran Subduction Zone," *Annu. Rev. Earth Planet. Sci.*, vol. 37, no. 1, pp. 345–366, Apr. 2009, doi: 10.1146/annurev.earth.031208.100212.

[7] H. Taubenböck *et al.*, "Risk Mitigation at the 'Last-Mile' -- From Science to Action by the Example of Padang, Indonesia," Jan. 2010.

[8] BPS Kabupaten Pesisir Selatan, *Kecamatan IV JURAI Dalam Angka*. 2022.

[9] D. Meitrya, "Kajian Tingkat Kerentanan Bangunan Akibat Gelombang Tsunami Berbasis Sistem Informasi Geografis (SIG)," Jakarta, 2021.

[10] Syamsidik, T. M. Rasyif, H. M. Fritz, Y. Idris, and I. Rusydy, "Fragility based characterization of alternative tsunami evacuation buildings in Banda Aceh, Indonesia," *Int. J. Disaster Risk Reduct.*, vol. 88, no. 8, p. 103607, 2022, doi: 10.1016/j.ijdrr.2023.103607.

[11] A. Muhari *et al.*, "Tsunami mitigation efforts with pTA in west Sumatra province, Indonesia," *J. Earthq. Tsunami*, vol. 4, no. 4, pp. 341–368, 2010, doi: 10.1142/S1793431110000790.

[12] Y. Fujii, K. Satake, S. Watada, and T.-C. Ho, "Slip distribution of the 2005 Nias earthquake (Mw 8.6) inferred from geodetic and far-field tsunami data," *Geophys. J. Int.*, vol. 223, pp. 1162–1171, Nov. 2020, doi: 10.1093/gji/ggaa384.

[13] I. R. Pranantyo, "ANALISIS PROBABILISTIK BAHAYA TSUNAMI KAWASAN LAUT BANDA," 2017. [Online]. Available: https://digilib.itb.ac.id/index.php/gdl/view/22501

[14] I. E. Mulia, T. Ishibe, K. Satake, A. R. Gusman, and S. Murotani, "Regional probabilistic tsunami hazard assessment associated with active faults along the eastern margin of the Sea of Japan," *Earth, Planets Sp.*, vol. 72, no. 1, 2020, doi: 10.1186/s40623-020-01256-5.

[15] I. Aida, "Reliability Of A Tsunami Source Model Derived From Fault Parameters," pp. 57–73, 1978.

[16] S. Koshimura, T. Oie, H. Yanagisawa, and F. Imamura, "Developing fragility functions for tsunami damage estimation using numerical model and post-tsunami data from banda aceh, Indonesia," *Coast. Eng. J.*, vol. 51, no. 3, pp. 243–273, 2009, doi: 10.1142/S0578563409002004.

[17] D. Febrianti and M. Safriani, "Kajian Tingkat Kerentanan Bangunan Terhadap Tsunami Dengan Metode BTV (Studi Kasus Pada Desa Kuta Padang, Kabupaten Aceh Barat)," *J. Tek. Sipil Fak. Tek. Univ. Teuku Umar*, vol. 2, no. 2477–5258, pp. 45–55, 2016.

[18] R. Omira, M. A. Baptista, J. M. Miranda, E. Toto, C. Catita, and J. Catalão, "Tsunami vulnerability assessment of Casablanca-Morocco using numerical modelling and GIS tools," *Nat. Hazards*, vol. 54, no. 1, pp. 75–95, 2010, doi: 10.1007/s11069-009-9454-4.

[19] P. M. Mai and G. C. Beroza, "A spatial random field model to characterize complexity in earthquake slip," *J. Geophys. Res. Solid Earth*, vol. 107, no. B11, p. ESE 10-1-ESE 10-21, 2002, doi: 10.1029/2001jb000588.